

Technical Report

# PAXgene-fixed paraffin-embedded sample is applicable to laser capture microdissection with well-balanced RNA quality and tissue morphology

Masaki Yamazaki<sup>1\*</sup>, Nami Yabuki<sup>1,2</sup>, Yasunori Suzuki<sup>2</sup>, Mayumi Ito<sup>2</sup>, Asuka Ikeda<sup>3</sup>, Osamu Natori<sup>2</sup>, Masami Suzuki<sup>1,2</sup>, and Atsuhiko Kato<sup>1</sup>

<sup>1</sup> Research Division, Chugai Pharmaceutical Co., Ltd., 1-135 Komakado, Gotemba-shi, Shizuoka 412-8513, Japan

<sup>2</sup> Forerunner Pharma Research Co., Ltd., Yokohama Bio Industry Center, 1-6 Suehiro-cho, Tsurumi-ku, Yokohama-shi, Kanagawa 230-0045, Japan

<sup>3</sup> Chugai Research Institute for Medical Science, Inc., 1-135, Komakado, Gotemba-shi, Shizuoka 412-8513, Japan

**Abstract** : Assessing how gene expression analysis by RNA sequencing (RNA-Seq) correlates to a unique morphology is increasingly necessary, and laser capture microdissection (LCM) is a critical research tool for discovering the genes responsible in a region of interest (ROI). Because RNA-Seq requires high-quality RNA, a sample preparation procedure that can preserve morphology and give the required quality of RNA is essential. A PAXgene®-fixed paraffin-embedded (XFPE) block can satisfy the need for high-quality RNA, but there are few reports on adapting the method for LCM, such as how small an ROI is analyzable by RNA-Seq. In this study, we confirmed the morphology and preservation of RNA in XFPE and then assessed the relationship between the size of pieces cut by LCM and their RNA quality. In XFPE, the morphology was similar to that in alcohol-based fixed samples, the quality of the RNA extracted from a whole sample was excellent, that is equivalent to that of a fresh frozen sample, and the quality was maintained over one year later. Three sizes of pieces—large (25,000  $\mu\text{m}^2$ ), medium (5,000  $\mu\text{m}^2$ ), and small (1,000  $\mu\text{m}^2$ )—were cut by LCM so that the total areas of the sections cut per size were the same. RNA quality was found to be best preserved when tissue was cut into pieces of over 5,000  $\mu\text{m}^2$ . In summary, XFPE exhibits good morphology and excellent preservation of RNA quality. Furthermore, it can be a good tool when used with LCM and RNA-Seq, giving well-balanced RNA quality and tissue morphology in the ROI. (DOI: 10.1293/tox.2017-0049; J Toxicol Pathol 2018; 31: 213–220)

**Key words**: PAXgene, RNA quality, morphology, laser capture microdissection, RNA-Seq

Recently, next-generation sequencing (NGS) technology is revolutionizing large-scale gene analysis and is supplanting microarrays as the technology of choice for quantifying and annotating transcriptomes<sup>1–3</sup>. Compared with microarrays, RNA-Sequencing (RNA-Seq) is better able to discover novel transcripts, identify alternatively spliced genes, detect allele-specific expression and poorly expressed genes, and provide good reproducibility of results between laboratories and across platforms<sup>4, 5</sup>. However, to ensure a successful RNA-Seq experiment, the quality of RNA must be sufficient to produce a library for sequencing and to allow appropriate biological conclusions to be made<sup>4</sup>.

At the same time, correlating a unique morphology with information on gene expression has come to be recognized as a way to decipher the details of disease biology in both clinical and preclinical studies<sup>6–10</sup>. Because laser capture microdissection (LCM) can isolate homogeneous cell subpopulations from complex tissues, genes responsible for disease onset and progression can be discovered more easily by evaluating gene expression in LCM samples than in whole homogenized samples. The majority of microdissection-based mRNA expression studies have been performed on frozen samples, in which traditional protocols for target collection, LCM slides, and lysis preparation ensure high RNA quality<sup>6–13</sup>, but morphology is not well preserved<sup>14</sup>. When unique morphology needs to be focused on in detail, some other method of preparing samples is needed to achieve a good balance of RNA quality and tissue morphology. In our group, this trade-off was solved for microarrays by using samples that are fixed in paraformaldehyde and then embedded in paraffin by the AMeX (acetone, methyl benzoate, and xylene) method (PFA-AMeX), which is a tool that provides good morphology and RNA quality and can also be combined with LCM<sup>15</sup>. Indeed, when the PFA-

Received: 15 August 2017, Accepted: 13 March 2018

Published online in J-STAGE: 12 April 2018

\*Corresponding author: M Yamazaki

(e-mail: yamazakimsk@chugai-pharm.co.jp)

©2018 The Japanese Society of Toxicologic Pathology

This is an open-access article distributed under the terms of the Creative Commons Attribution Non-Commercial No Derivatives

(by-nc-nd) License. (CC-BY-NC-ND 4.0: <https://creativecommons.org/licenses/by-nc-nd/4.0/>).



AMeX method is used, morphological preservation is excellent, and RNA quality is modestly better than 10% neutral buffer formalin-fixed paraffin-embedded (FFPE) samples. However, RNA extracted from PFA-AMeX samples shows no peaks of 18 s and 28 s, which indicates that substantial degradation of RNA occurs, and therefore the method is not suitable for RNA-Seq.

Samples prepared by a novel formalin-free fixation technology, PAXgene® (Qiagen GmbH, Hilden, Germany), and then embedded in paraffin (XFPE) simultaneously preserve tissue morphology and antigenicity as well as nucleic acids, proteins, and phosphoproteins<sup>16–23</sup>, and their morphology was appropriate for diagnosing clinical colon cancer samples in an international ring trial<sup>23</sup>. Compared with formalin, the PAXgene fixative uses a non-cross-linking, non-carcinogenic mixture of different alcohols, acids, and a soluble organic compound that rapidly preserves the morphology as well as all the biomolecules.

Combining XFPE and LCM may allow RNA-Seq to give appropriate biological insights by providing a good balance between RNA quality and tissue morphology in a region of interest (ROI). As far as we know, only one report has been published about adapting XFPE to microdissection for DNA and RNA analysis<sup>24</sup>, but in that study whole peripapillary retina was dissected into 2 mm sections using a 27-gauge needle with a beveled tip, which is too large to correctly evaluate the influence of cutting small pieces of a sample. To focus on the ROI in detail, it is important to know how small a piece of an XFPE sample cut by LCM is acceptable for RNA-Seq, but no report has been published. Thus, we attempted to study the characteristics of XFPE by comparing the morphology and preservation of RNA with that in other block preparation procedures and evaluating the relationship between the size of the pieces cut by LCM and the RNA quality.

Three SCID mice (CB17/Icr-Prkdc<sup>scid</sup>/CrjCrlj) were purchased from Charles River Laboratories Japan, Inc. (Kanagawa, Japan), and used in experiments at around 8 weeks of age. The animals were housed in cages in an animal room maintained at a temperature of  $24 \pm 2^\circ\text{C}$  and a humidity of  $55 \pm 10\%$ , with 14 to 16 air changes per h and a 14-h light and 10-h dark cycle. The animals were given pelleted chow (Gamma-Irradiated CF, Oriental Yeast Co., Ltd., Tokyo, Japan) and sterilized water ad libitum. All animal procedures were conducted in accordance with Forerunner Pharma Research's Guide for the Care and Use of Laboratory Animals, and all experimental protocols were approved by the Institutional Animal Care and Use Committee.

The human colorectal cancer cell line HCT116 was obtained from the European Collection of Authenticated Cell Cultures (ECACC, Salisbury, UK) and cultured in McCoy's 5a medium (Invitrogen/Thermo Fisher Scientific, Waltham, MA, USA) supplemented with 10% (v/v) fetal bovine serum. The HCT116 cells ( $1 \times 10^6$ ) were suspended in 50% Matrigel (Becton, Dickinson and Company, Franklin Lakes, NJ, USA) and inoculated subcutaneously into the flanks of the mice.

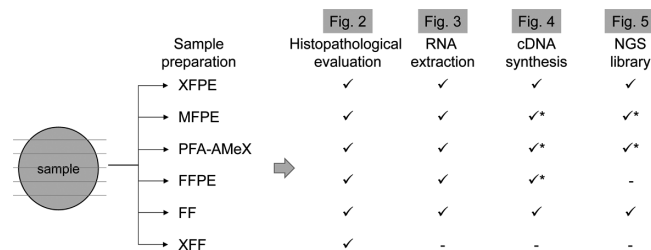


**Fig. 1.** Experimental design for block preparation, histopathological evaluation, RNA extraction, cDNA synthesis, and NGS library synthesis. XFPE, PAXgene-fixed paraffin-embedded; MFPE, modified methacarn-fixed paraffin-embedded; PFA-AMeX, paraformaldehyde-fixed paraffin-embedded using the AMeX method; FFPE, formalin-fixed paraffin-embedded; FF, fresh frozen; XFF, PAXgene-fixed frozen; ✓, conducted; -, not conducted. An asterisk denotes that a sample with the highest RIN was used.

The HCT116 xenograft mice were sacrificed by exsanguination under deep anesthesia approximately three weeks after inoculation. Each of the xenograft samples and livers were taken and divided into six pieces. The liver was selected as an organ large enough to divide into six pieces. Pieces of each tissue were prepared by processing them in the following ways: as XFPE, modified methacarn-fixed paraffin-embedded (MFPE), PFA-AMeX, FFPE, fresh-frozen (FF), and PAXgene®-fixed frozen (XFF) blocks (Fig. 1).

For XFPE, samples were fixed at room temperature in the fixative in Chamber 1 of a PAXgene Tissue Container (Qiagen). Fixation was stopped after 3 h, and samples were transferred into the stabilizer reagent in Chamber 2 of the same PAXgene Tissue Container (Qiagen) and immersed continuously for 24 h. After fixation, the samples were immersed in 80%, 90%, 100%, and 100% ethanol (1 h each), subjected to 2 changes of xylene after 1 h each at room temperature, and finally submerged in paraffin with a low melting point (Paraplast X-TRA®, Merck KGaA, Darmstadt, Germany) at  $56^\circ\text{C}$  for 2 h, according to the manufacturer's instructions. For XFF, samples fixed and stabilized by PAXgene reagents with the same procedure as described above were embedded into O.C.T. Compound (Sakura Finetek Japan Co., Ltd., Tokyo, Japan) after dehydration in 10%, 15%, and 20% sucrose for 4 h, 4 h, and overnight, respectively. For MFPE, samples were immersed into modified methacarn fixative (methanol:glacial acetic acid = 8:1)<sup>14</sup> for 24 h at room temperature, and the standard procedure was followed. For FF, tissues were directly embedded in O.C.T. Compound and fixed by dry ice/acetone-cooled hexane. For FFPE, tissues were fixed in 10% neutral buffer formalin (pH 7.4) for 24 h at room temperature and embedded in paraffin wax following conventional procedures. Finally for PFA-AMeX, tissues were fixed in 4% paraformaldehyde in phosphate buffer for 24 h at  $4^\circ\text{C}$  and embedded into paraffin using the AMeX method<sup>25</sup>. The XFPE block was stored at  $-30^\circ\text{C}$  following the manufacturer's instruction, the FF and XFF blocks were stored at  $-80^\circ\text{C}$ , the PFA-AMeX block

was stored at 4°C, and the MFPE and FFPE blocks were stored at room temperature. Sections from each block were stained with hematoxylin and eosin (HE) and histopathologically evaluated under light microscopy.

XFPE, MFPE, PFA-AMeX, FFPE, and FF blocks from liver samples were sectioned into two slices (each 10 µm thick) approximately three months after collection and transferred to a microcentrifuge tube, in which RNA was extracted using a PAXgene® Tissue miRNA Kit (Qiagen) for XFPE, an miRNeasy FFPE Kit (Qiagen) for MFPE, PFA-AMeX, and FFPE, and an miRNeasy Micro Kit (Qiagen) for FF, according to the manufacturer's instructions. For XFPE, RNA was eluted with RNase-free water instead of Buffer TR4. As for the XFF, RNA quality was not evaluated in a whole section of sample because histopathological evaluation of the tissue-processing method confirmed that the morphology was not preserved. The RNA Integrity Number (RIN) and yield of extracted total RNAs were assessed using an Agilent Bioanalyzer 2100 system with an RNA 6000 Pico Kit (Agilent Technologies, Santa Clara, CA, USA) and Quant-iT™ RiboGreen® RNA Assay Kit (Invitrogen/Thermo Fisher Scientific, Waltham, MA, USA) according to the manufacturers' instructions. The RIN is commonly used to evaluate the quality of RNA and is calculated by the 28S peak area divided by the 18S peak area and an undisclosed variable<sup>26</sup>. RIN values range from 10 (intact) to 1 (totally degraded). The gradual degradation of rRNA is reflected by a continuous shift towards shorter fragment sizes. A RIN value over 6.0 could be considered high quality<sup>4, 27</sup>. cDNA was synthesized with a SMART-Seq® v4 Ultra® Low Input RNA Kit for Sequencing (Clontech Laboratories, Inc., CA, USA) from 1 ng total RNA input. An NGS library was prepared with a Nextera XT DNA Library Preparation Kit (Illumina, Inc., San Diego, CA, USA) from 200 pg cDNA input according to the manufacturer's instructions. The obtained NGS library was sequenced on an Illumina Next-Seq500 sequencer generating 2 × 75-bp paired-end reads. Raw sequence data was processed to obtain mapping and gene expression data using the Illumina BaseSpace® Onsite pipeline, which was also used to generate a gene body coverage plot. Gene body coverage is a metric for assessing the quality of RNA-Seq data and shows the percentage of reads covering each nucleotide position for all genes scaled to 100 bins<sup>28</sup>. Correlation of the gene expression between XFPE, FF, PFA-AMeX, and MFPE was assessed using Pearson's coefficient of correlation. To assess the influence of long-term storage of XFPE blocks, the quality of extracted RNA was also evaluated over one year later by the same protocol as that described above in whole sections taken from the same blocks.

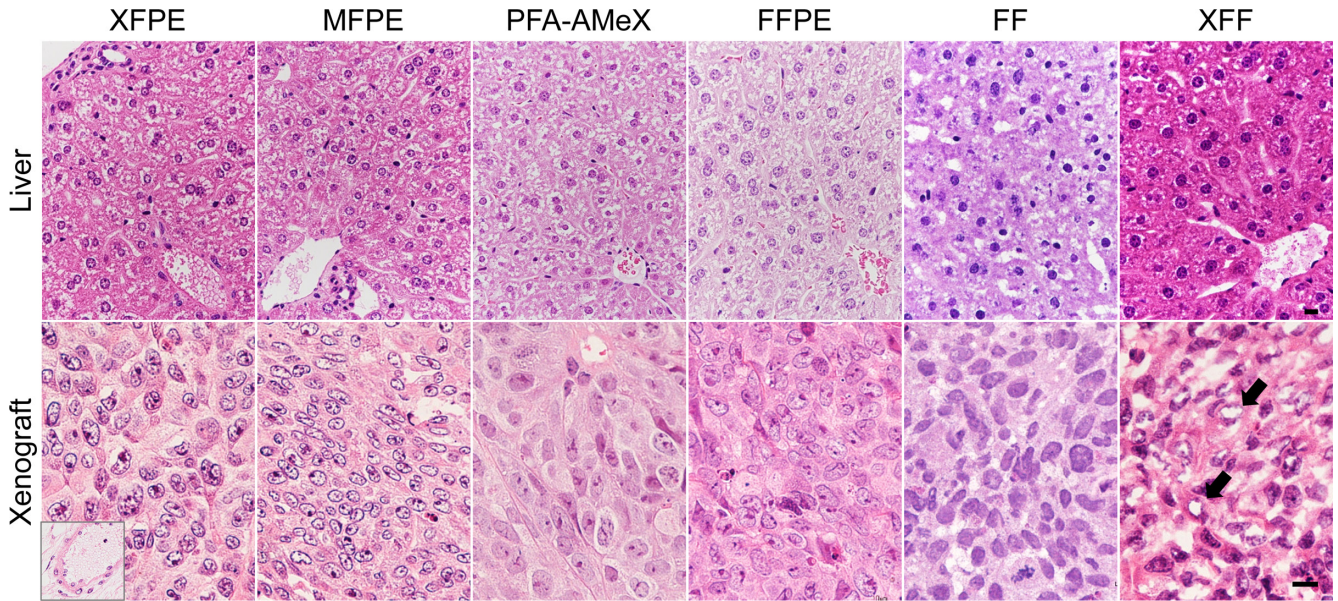
For LCM, XFPE blocks from HCT116 xenograft samples were sectioned (6 µm thick) at room temperature, floated in an RNase-free water bath, and transferred to FrameSlides® (Leica Microsystems, Wetzlar, Germany). HCT116 was selected to study the relationship between cutting size and RNA quality because we wanted to reduce the influence of tissue type on RNA quality, and HCT116 tissue

is considered to be more homogeneous than that of other normal organs. After being stained with HE, pieces were cut by Leica LMD7000 (Leica Microsystems) into three different sizes, namely, small (990–1,010 µm<sup>2</sup>), medium (4,900–5,100 µm<sup>2</sup>), and large (24,900–25,100 µm<sup>2</sup>). A sufficient number of pieces of each size were cut so that the total area for each size was approximately 400,000 µm<sup>2</sup>, which had been confirmed in a preliminary study as yielding sufficient RNA to perform RNA-Seq. The object lens was set at ×10 and the laser power, aperture, and speed parameters of the LMD7000 were configured at 30, 18, and 7, respectively. Total RNA was extracted from each microdissected sample using a PAXgene® Tissue miRNA Kit (Qiagen) following the manufacturer's supplementary protocol for microdissected tissues. The RIN and yield of extracted total RNAs were assessed using an Agilent Bioanalyzer 2100 system (Agilent Technologies) and Quant-iT™ RiboGreen® RNA Assay Kit (Invitrogen/Thermo Fisher Scientific) according to the manufacturers' instructions.

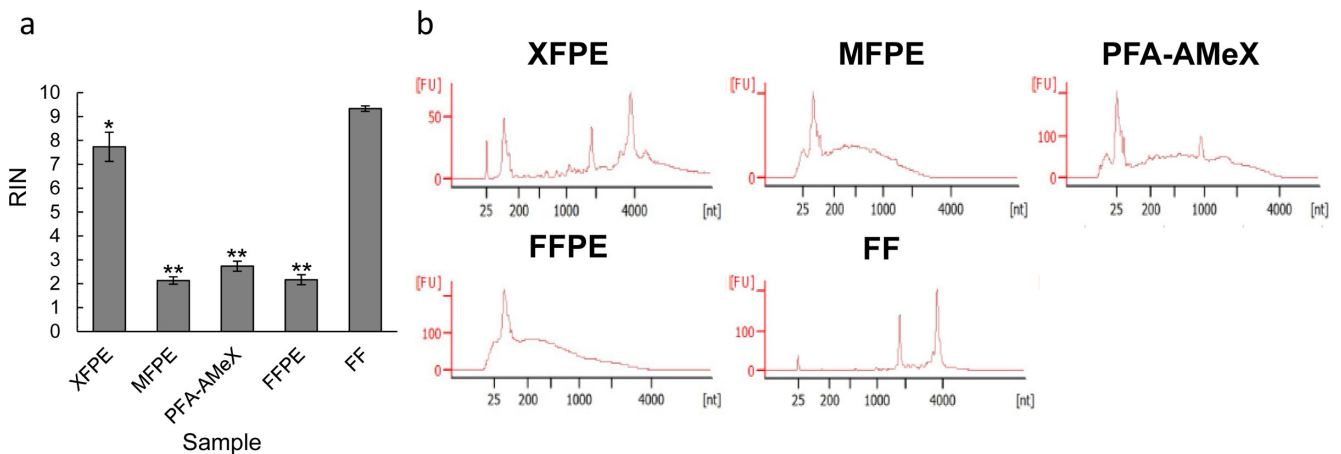
All mean values are reported as the mean ± standard deviation value. Welch's *t* test was used to determine the significance of differences between groups. *P* values of <0.05 or <0.01 were considered significant.

Figure 2 shows a comparison of the morphology in HE section slides made according to each preparation procedure. Cell shrinkage, slightly eosinophilic cytoplasm, coarse chromatin pattern, prominent nucleolus, and ghosted red blood cells were observed for XFPE, but the cell shape was preserved, and each cell was clearly distinguishable. MFPE showed almost the same morphology as XFPE, in that cell shrinkage, a coarse chromatin pattern, a prominent nucleolus, and ghosted red blood cells were observed. PFA-AMeX and FFPE showed no shrinkage of cells and no coarse chromatin in nuclei, and the cell border was very clear. The border between cells in the frozen section was ambiguous, and the nucleolus was not recognizable. In XFF samples, many artificial vacuoles were observed in the cells, and the cell border was ambiguous.

RNA quality in blocks prepared by each procedure was compared in whole sections from liver samples three months after collection (*n*=3, respectively) (Fig. 3a and b). The bad morphology of XFF made it pointless to pursue comparing the RNA quality. FF also showed bad morphology, but we used it as a reference for high RNA quality when comparing the RNA quality of other block preparation procedures. Though extracted from roughly the same size of liver samples, the RNA yield from FF was lower than from the other block preparation procedures (258–453 ng). XFPE, PFA-AMeX, MFPE, and FFPE showed an RNA yield of roughly over 1,000 ng. The RIN value of XFPE (7.7 ± 0.6) was lower than that of FF (9.3 ± 0.1), but that of XFPE was still over 6.0. Furthermore, those of the other block preparation procedures were significantly lower than that of FF. Figure 3b shows typical capillary electropherograms of rRNA from the different block preparation procedures, with 28S/18S rRNA ratios of 2.2 ± 0.3, 0.3 ± 0.5, 0.1 ± 0.1, 0 ± 0, and 1.4 ± 0.1 for XFPE, MFPE, PFA-AMeX, FFPE, and FF, respec-



**Fig. 2.** Histopathological evaluation of liver and xenograft tissue processed by each block preparation procedure. Inset, ghosted red blood cells in blood vessel. Arrow, vacuoles observed in XFF. HE staining. Bar = 10  $\mu$ m.



**Fig. 3.** RNA quality of whole sections of liver samples measured by a bioanalyzer. (a) RIN value for whole sections of liver samples processed by each block preparation procedure (n=3). \*P<0.05 compared with the FF group. \*\*P<0.01 compared with the FF group. (b) Typical capillary electropherograms of rRNA from each block preparation procedure.

tively. In FF and XFPE, the rRNA peak was visible at both 18 s and 28 s, PFA-AMeX showed only a slight 18 s peak, and MFPE and FFPE had a broad pattern with a progressive disappearance of 18 s and 28 s.

cDNA was synthesized from XFPE and FF blocks (n=3, respectively). PFA-AMeX and MFPE blocks with the highest RIN values out of three were synthesized for reference. Although cDNA synthesis was attempted in FFPE, cDNA could not be synthesized. The cDNA yield from XFPE ( $4.8 \pm 0.7$  ng; range, 4.3–5.6 ng) was significantly lower than that from FF ( $10.6 \pm 2.5$  ng; range, 8.1–13.0 ng) (Fig. 4a). In the gene body coverage plot, the FF coverage was fairly even through 3' to 5'. The coverage of XFPE was slightly biased to

3' but very similar to that of FF (n=3, respectively) (Fig. 4b). On the other hand, PFA-AMeX and MFPE produced reads heavily biased to 3' (n=1, respectively). Because modified oligo-dT was used for reverse transcription, the heavy bias to 3' suggests degradation of the original total RNA. An NGS library was prepared from 200 pg cDNA input with a Nextera XT DNA Library Preparation Kit. The average size of the NGS library from XFPE (530–572 bp) was slightly smaller than that from FF (583–721 bp) (Fig. 5a), and the library yield from XFPE (35.1–46.7 ng) was almost the same as that from FF (34.9–46.2 ng) (Fig. 5b). The correlation coefficients for gene expression from FF, XFPE, PFA-AMeX, and MFPE were checked (Fig. 5c). The value of the correla-

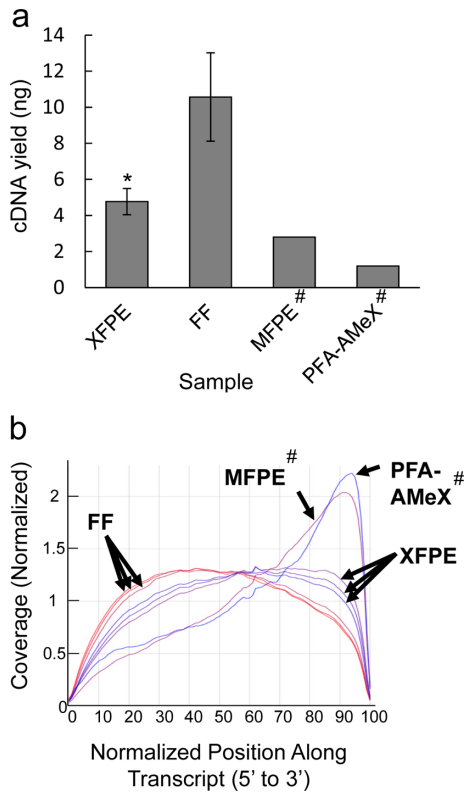


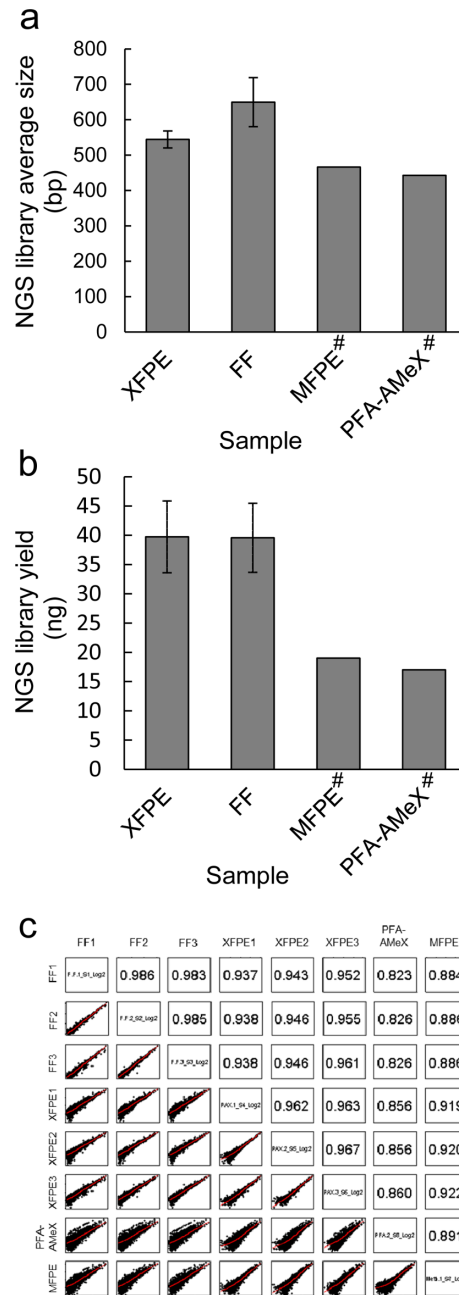
**Fig. 4.** Quality and quantity check for cDNA. (a) cDNA yield from each block preparation procedure. \* $P < 0.05$  compared with the FF group. #The sample with the highest RIN was used. (b) Gene body coverage of FF, XFPE ( $n=3$ , respectively), PFA-AMeX, and MFPE ( $n=1$ , respectively). #The sample with the highest RIN was used. The vertical axis shows the normalized read coverage over each nucleotide position of all of the genes, and the horizontal axis shows each nucleotide position of all of the genes scaled to 100 bins from 5' to 3'.

tion coefficient between FF and XFPE ranged from 0.937 to 0.961, but for PFA-AMeX and MFPE, the correlation coefficient against FF ranged from 0.823 to 0.886.

Table 1 shows the influence of long-term storage on XFPE blocks by comparing the RNA quality at three months with that in the same blocks after one year. The quality of RNA data at three months (as seen in Fig. 3) decreased after one year, as shown by the RIN value, which decreased from 7.2–8.4 to 6.2–6.7.

The relationship between the size of LCM pieces and RNA quality was assessed from xenograft samples (Fig. 6a). Large-, medium-, and small-sized pieces were cut, ensuring that the total area of the pieces cut was 400,000  $\mu\text{m}^2$  for each size ( $n=3$ , respectively). The RIN values of the large- and small-sized pieces were significantly decreased compared with the whole sectioned sample, but the large- and medium- sized pieces still showed RNA values of over 6.0 (Fig. 6b).

Though it is increasingly necessary to assess how gene expression analyzed by RNA-Seq correlates to a unique morphology in a ROI<sup>6–13</sup>, standard pathological sample pro-

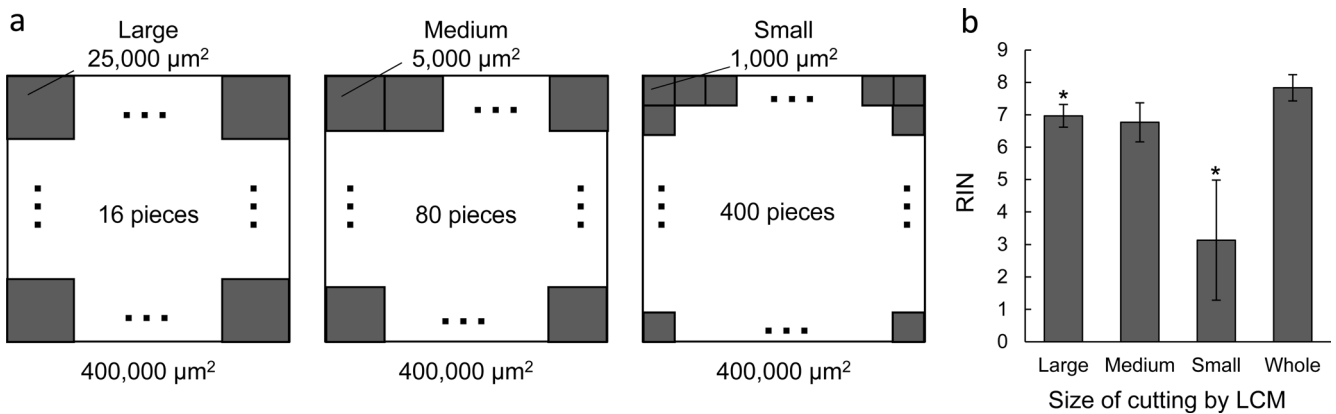


**Fig. 5.** Quality and quantity check for NGS libraries. (a) Average size of the NGS library from each block preparation procedure. (b) NGS library yield from each block preparation procedure. (c) Scatter plots and the values of correlation coefficients for gene expression from FF, XFPE ( $n=3$ , respectively), PFA-AMeX, and MFPE ( $n=1$ , respectively). #The sample with the highest RIN was used.

cedures like FFPE and FF provide only one aspect: either good morphology or well-preserved RNA<sup>14, 17, 29</sup>. The problem of trade-off needs to be solved, and a novel sample preparation procedure that can preserve morphology and give good quality RNA has become essential. Though XFPE was one solution to the problem, there have been few reports on adapting XFPE for LCM, and especially, there has been no

**Table 1.** The Influence of Long-term Storage on XFPE Blocks by Comparing the RNA Quality at Three Months with That in the Same Blocks after One Year

Sample	3 month			Over 1 year		
	RNA yield (ng)	RIN	rRNA Ratio (28 s/18 s)	RNA yield (ng)	RIN	rRNA Ratio (28 s/18 s)
1	1,220	7.2	2.2	1,122	6.5	0.7
2	2,616	7.6	1.9	1,753	6.2	0.6
3	1,633	8.4	2.5	1,630	6.7	0.7

**Fig. 6.** Relationship between size of LCM pieces and RNA quality. (a) Schematic image of LCM. A size (large, medium, or small) was assigned to each section, and a sufficient number of pieces was cut to ensure a total area of approximately 400,000  $\mu\text{m}^2$  per size. (b) Relationship between size and RIN value in XFPE xenograft samples ( $n=3$ ). Whole sections of sample were examined as a reference ( $n=3$ ). \* $P<0.05$  compared with the whole sections.

information on how small a ROI could be analyzed by RNA-Seq. In this study, we assessed the characteristics of XFPE and attempted to apply the procedure to LCM.

Regarding the morphological features in XFPE, cell shrinkage, eosinophilic cell cytoplasm, and ghosted red blood cells were observed and were similar to those previously reported for alcohol-based fixatives<sup>17, 19, 30</sup>, which are generally known to be acceptable<sup>31</sup>, and cells themselves and cell-cell border could be seen in detail in XFPE, just as they can in other alcohol-based fixatives. However, some researchers have pointed out differences between XFPE and FFPE in the immunohistochemistry staining patterns<sup>30, 32</sup> of some common targets, like CCND1, Ki67, and c-kit<sup>33</sup>. Thus, it is better to consider XFPE as a secondary sample to FFPE when examining the morphology.

In contrast, RNA preservation in XFPE was excellent compared with samples made by other preparation procedures, including PFA-AMeX and MFPE, which are both known as preparation procedures that highly preserve RNA<sup>14, 15</sup>, though there is no report that directly compares them with XFPE. Other than FF, only XFPE provided a quality of RNA high enough to merit proceeding to RNA-Seq analysis, and XFPE can be a substitute for FF. The RNA quality was sufficient to generate an NGS library of appropriate size and sufficient yield, and furthermore, the gene expression from XFPE showed a higher correlation coefficient with FF than PFA-AMeX and MFPE did.

This study found that LCM could be used on XFPE blocks. When a small ROI is the target of RNA-Seq, pathologists must collect small pieces with the same morphological features that total an area sufficient for performing RNA-Seq. When the pieces cut by LCM were larger than 5,000  $\mu\text{m}^2$ , RIN value of more than 6.2 could be preserved, which was lower than in a whole section. Meanwhile, the RIN value was lower than 6.0 when the pieces were cut at 1,000  $\mu\text{m}^2$ . Though the time taken for microdissection is known to also affect RNA quality<sup>9</sup>, the time for microdissection of one sample was less than 30 min in this study. In general, 30 min has no influence on RNA quality when microdissection is conducted on formalin-, paraformaldehyde-, or glutaraldehyde-fixed tissue<sup>9</sup>, so size was thought to be the most influential factor in preserving RNA quality. RNA is known to be damaged by heat and UV light<sup>9, 27</sup>, and the LCM system we used in this study was powered by a UV laser, so the smallest size may not have been acceptable because a large area of the piece was touched by the laser. An infrared laser causes less damage to tissue<sup>9</sup>, so the RNA in samples cut by infrared LCM may be better preserved even at the smallest size. Based on the results of this study, each researcher should determine the size of the pieces cut from XFPE blocks by LCM according to the purpose of the study.

Although the RIN value of XFPE after one year was slightly lower than at three months, it was still higher than 6.0. Whereas the manufacturer's instructions state that there

is no effect on the morphology and integrity of the nucleic acids for up to 3 months of storage at  $-30^{\circ}\text{C}$ , this study shows that it is possible to maintain the quality of RNA for longer. However, the study also shows that LCM results in a reduction in RNA quality. Therefore, in the view of the authors, researchers that intend to use LCM on an XFPE block stored for one year should first check the RNA quality in whole sections of the sample and calculate the overall effect of storage and LCM on RNA quality.

In conclusion, XFPE provides samples with a good balance of RNA quality and tissue morphology that can be dissected by LCM for RNA-Seq in the ROI. This method will be particularly useful for harmonizing morphological evaluation and large-scale gene analysis.

**Disclosure of Potential Conflicts of Interest:** The authors declare that they have no competing interests.

**Acknowledgments:** We thank Dr. Takeshi Watanabe at Chugai Research Institute for Medical Science for his technical support and discussion.

## References

- Goodwin S, McPherson JD, and McCombie WR. Coming of age: ten years of next-generation sequencing technologies. *Nat Rev Genet.* **17**: 333–351. 2016. [[Medline](#)] [[CrossRef](#)]
- Mardis ER. Next-generation sequencing platforms. *Annu Rev Anal Chem (Palo Alto, Calif).* **6**: 287–303. 2013. [[Medline](#)] [[CrossRef](#)]
- Mortazavi A, Williams BA, McCue K, Schaeffer L, and Wold B. Mapping and quantifying mammalian transcripts by RNA-Seq. *Nat Methods.* **5**: 621–628. 2008. [[Medline](#)] [[CrossRef](#)]
- Kukurba KR, and Montgomery SB. RNA Sequencing and Analysis. *Cold Spring Harb Protoc.* **2015**: 951–969. 2015. [[Medline](#)] [[CrossRef](#)]
- Ledford H. The death of microarrays? *Nature.* **455**: 847. 2008. [[Medline](#)] [[CrossRef](#)]
- Castro NP, Merchant AS, Saylor KL, Anver MR, Salomon DS, and Golubeva YG. Adaptation of Laser Microdissection Technique for the Study of a Spontaneous Metastatic Mammary Carcinoma Mouse Model by NanoString Technologies. *PLoS One.* **11**: e0153270. 2016. [[Medline](#)] [[CrossRef](#)]
- Ma X-J, Dahiya S, Richardson E, Erlander M, and Sgroi DC. Gene expression profiling of the tumor microenvironment during breast cancer progression. *Breast Cancer Res.* **11**: R7. 2009. [[Medline](#)] [[CrossRef](#)]
- Espina V, Heiby M, Pierobon M, and Liotta LA. Laser capture microdissection technology. *Expert Rev Mol Diagn.* **7**: 647–657. 2007. [[Medline](#)] [[CrossRef](#)]
- Espina V, Wulfkühle JD, Calvert VS, VanMeter A, Zhou W, Coukos G, Geho DH, Petricoin EF 3rd, and Liotta LA. Laser-capture microdissection. *Nat Protoc.* **1**: 586–603. 2006. [[Medline](#)] [[CrossRef](#)]
- Erickson HS, Albert PS, Gillespie JW, Rodriguez-Canales J, Marston Linehan W, Pinto PA, Chuaqui RF, and Emmert-Buck MR. Quantitative RT-PCR gene expression analysis of laser microdissected tissue samples. *Nat Protoc.* **4**: 902–922. 2009. [[Medline](#)] [[CrossRef](#)]
- Baldelli E, Haura EB, Crinò L, Cress DW, Ludovini V, Schabath MB, Liotta LA, Petricoin EF, and Pierobon M. Impact of upfront cellular enrichment by laser capture microdissection on protein and phosphoprotein drug target signaling activation measurements in human lung cancer: Implications for personalized medicine. *Proteomics Clin Appl.* **9**: 928–937. 2015. [[Medline](#)] [[CrossRef](#)]
- Emmert-Buck MR, Bonner RF, Smith PD, Chuaqui RF, Zhuang Z, Goldstein SR, Weiss RA, and Liotta LA. Laser capture microdissection. *Science.* **274**: 998–1001. 1996. [[Medline](#)] [[CrossRef](#)]
- Jaquet R, Hillyer J, and Landis WJ. Analysis of connective tissues by laser capture microdissection and reverse transcriptase-polymerase chain reaction. *Anal Biochem.* **337**: 22–34. 2005. [[Medline](#)] [[CrossRef](#)]
- Cox ML, Schray CL, Luster CN, Stewart ZS, Korytko PJ, M Khan KN, Paulauskis JD, and Dunstan RW. Assessment of fixatives, fixation, and tissue processing on morphology and RNA integrity. *Exp Mol Pathol.* **80**: 183–191. 2006. [[Medline](#)] [[CrossRef](#)]
- Watanabe T, Kato A, Terashima H, Matsubara K, Chen YJ, Adachi K, Mizuno H, and Suzuki M. The PFA-AMeX method achieves a good balance between the morphology of tissues and the quality of RNA content in DNA microarray analysis with laser-capture microdissection samples. *J Toxicol Pathol.* **28**: 43–49. 2015. [[Medline](#)] [[CrossRef](#)]
- Ergin B, Meding S, Langer R, Kap M, Viertler C, Schott C, Ferch U, Riegman P, Zatloukal K, Walch A, and Becker KF. Proteomic analysis of PAXgene-fixed tissues. *J Proteome Res.* **9**: 5188–5196. 2010. [[Medline](#)] [[CrossRef](#)]
- Groelz D, Sobin L, Branton P, Compton C, Wyrich R, and Rainen L. Non-formalin fixative versus formalin-fixed tissue: a comparison of histology and RNA quality. *Exp Mol Pathol.* **94**: 188–194. 2013. [[Medline](#)] [[CrossRef](#)]
- Gündisch S, Schott C, Wolff C, Tran K, Beese C, Viertler C, Zatloukal K, and Becker KF. The PAXgene® tissue system preserves phosphoproteins in human tissue specimens and enables comprehensive protein biomarker research. *PLoS One.* **8**: e60638. 2013. [[Medline](#)] [[CrossRef](#)]
- Kap M, Smedts F, Oosterhuis W, Winther R, Christensen N, Reischauer B, Viertler C, Groelz D, Becker KF, Zatloukal K, Langer R, Slotta-Huspenina J, Bodo K, de Jong B, Oelmüller U, and Riegman P. Histological assessment of PAXgene tissue fixation and stabilization reagents. *PLoS One.* **6**: e27704. 2011. [[Medline](#)] [[CrossRef](#)]
- Oetjen J, Aichler M, Trede D, Strehlow J, Berger J, Heldmann S, Becker M, Gottschalk M, Kobarg JH, Wirtz S, Schiffler S, Thiele H, Walch A, Maass P, and Alexandrov T. MRI-compatible pipeline for three-dimensional MALDI imaging mass spectrometry using PAXgene fixation. *J Proteomics.* **90**: 52–60. 2013. [[Medline](#)] [[CrossRef](#)]
- Staff S, Kujala P, Karhu R, Rökman A, Ilvesaro J, Kares S, and Isola J. Preservation of nucleic acids and tissue morphology in paraffin-embedded clinical samples: comparison of five molecular fixatives. *J Clin Pathol.* **66**: 807–810. 2013. [[Medline](#)] [[CrossRef](#)]
- Viertler C, Groelz D, Gündisch S, Kashofer K, Reischauer B, Riegman PH, Winther R, Wyrich R, Becker KF, Oelmüller U, and Zatloukal K. A new technology for stabilization

- of biomolecules in tissues for combined histological and molecular analyses. *J Mol Diagn*. **14**: 458–466. 2012. [[Medline](#)] [[CrossRef](#)]
23. Gündisch S, Slotta-Huspenina J, Verderio P, Ciniselli CM, Pizzamiglio S, Schott C, Drecoll E, Viertler C, Zatloukal K, Kap M, Riegman P, Esposito I, Specht K, Babaryka G, Asslaber M, Bodó K, den Bakker M, den Hollander J, Fend F, Neumann J, Reu S, Perren A, Langer R, Lugli A, Becker I, Richter T, Kayser G, May AM, Carneiro F, Lopes JM, Sobin L, Höfler H, and Becker KF. Evaluation of colon cancer histomorphology: a comparison between formalin and PAXgene tissue fixation by an international ring trial. *Virchows Arch*. **465**: 509–519. 2014. [[Medline](#)] [[CrossRef](#)]
  24. Liu Y, and Edward DP. Assessment of PAXgene fixation on preservation of morphology and nucleic acids in microdissected retina tissue. *Curr Eye Res*. **42**: 104–110. 2017. [[Medline](#)] [[CrossRef](#)]
  25. Suzuki M, Katsuyama K, Adachi K, Ogawa Y, Yorozu K, Fujii E, Misawa Y, and Sugimoto T. Combination of fixation using PLP fixative and embedding in paraffin by the AMeX method is useful for histochemical studies in assessment of immunotoxicity. *J Toxicol Sci*. **27**: 165–172. 2002. [[Medline](#)] [[CrossRef](#)]
  26. Schroeder A, Mueller O, Stocker S, Salowsky R, Leiber M, Gassmann M, Lightfoot S, Menzel W, Granzow M, and Ragg T. The RIN: an RNA integrity number for assigning integrity values to RNA measurements. *BMC Mol Biol*. **7**: 3. 2006. [[Medline](#)] [[CrossRef](#)]
  27. Wang S, Wang L, Zhu T, Gao X, Li J, Wu Y, and Zhu H. Improvement of tissue preparation for laser capture microdissection: application for cell type-specific miRNA expression profiling in colorectal tumors. *BMC Genomics*. **11**: 163. 2010. [[Medline](#)] [[CrossRef](#)]
  28. Li S, Łabaj PP, Zumbo P, Sykacek P, Shi W, Shi L, Phan J, Wu PY, Wang M, Wang C, Thierry-Mieg D, Thierry-Mieg J, Kreil DP, and Mason CE. Detecting and correcting systematic variation in large-scale RNA sequencing data. *Nat Biotechnol*. **32**: 888–895. 2014. [[Medline](#)] [[CrossRef](#)]
  29. Dotti I, Bonin S, Basili G, Nardon E, Balani A, Siracusano S, Zanconati F, Palmisano S, De Manzini N, and Stanta G. Effects of formalin, methacarn, and fineFIX fixatives on RNA preservation. *Diagn Mol Pathol*. **19**: 112–122. 2010. [[Medline](#)] [[CrossRef](#)]
  30. Mathieson W, Marcon N, Antunes L, Ashford DA, Betsou F, Frasilho SG, Kofanova OA, McKay SC, Pericleous S, Smith C, Unger KM, Zeller C, and Thomas GA. A Critical Evaluation of the PAXgene Tissue Fixation System: Morphology, Immunohistochemistry, Molecular Biology, and Proteomics. *Am J Clin Pathol*. **146**: 25–40. 2016. [[Medline](#)] [[CrossRef](#)]
  31. Milcheva R, Janega P, Celec P, Russev R, and Babál P. Alcohol based fixatives provide excellent tissue morphology, protein immunoreactivity and RNA integrity in paraffin embedded tissue specimens. *Acta Histochem*. **115**: 279–289. 2013. [[Medline](#)] [[CrossRef](#)]
  32. Belloni B, Lambertini C, Nuciforo P, Phillips J, Bruening E, Wong S, and Dummer R. Will PAXgene substitute formalin? A morphological and molecular comparative study using a new fixative system. *J Clin Pathol*. **66**: 124–135. 2013. [[Medline](#)] [[CrossRef](#)]
  33. Furukawa S, Nagaike M, and Ozaki K. Databases for technical aspects of immunohistochemistry. *J Toxicol Pathol*. **30**: 79–107. 2017. [[Medline](#)] [[CrossRef](#)]